MEASURING THE INFLUENCE OF A MOTORWAY CONSTRUCTION ON LAND SURFACE TEMPERATURE USING LANDSAT THERMAL DATA: A CASE STUDY IN THE METROPOLITAN CITY OF MILAN

A. Vavassori[1]*, M. Puche[1], M. A. Brovelli[1]

[1] Dept. of Civil and Environmental Engineering, Politecnico di Milano, P.zza Leonardo da Vinci 32, 20133 Milano, Italy - (alberto.vavassori, maria.brovelli)@polimi.it, mathildedanielle.puche@mail.polimi.it

KEY WORDS: Motorway construction, Land Surface Temperature, Landsat, Urban Heat Island, Remote Sensing

ABSTRACT:

Cities have been identified as a landmark for climate change, being among the direct targets of its negative feedbacks. The combined effect of climate change and rapidly growing urbanization is exacerbating the urban heat island phenomenon in cities worldwide. The availability of multiple geo-data sources including satellite remote sensing products is significantly empowering the investigation of its driving factors. This is a crucial step to implement ad hoc mitigation and adaptation strategies. In view of the above, the goal of this study is to measure the effect of a motorway on the Land Surface Temperature (LST) space-time patterns by leveraging Landsat 5 and 8 thermal data of the period from 2006 to 2022. The study area is around the motorway A58 and connected roads in the Metropolitan City of Milan (northern Italy). LST patterns are investigated along the motorway track and in the neighbouring areas before and after the motorway construction, in both the cold and warm seasons. Results show that the motorway significantly affects the LST distribution during summer with a median increase of 2.5°C along the road track with respect to the surrounding area. The warming effect is also recorded in the road buffers with decreasing LST with increasing distance from the road. On the contrary, no meaningful variation in terms of LST is measured in winter. These experiments provide insightful measures of the effect of a highway on the local climate conditions in an urban area, thus representing crucial pieces of information for driving evidence-based urban planning activities.

1. INTRODUCTION

Cities host nowadays 55% of the total world's population and this number is expected to rise to 66% by 2050 (United Nations, 2018). Urban areas concentrate people, human activities, and strategical assets while generating more than 80% of the global Gross Domestic Product (GDP), which makes them a benchmark for the global economy (World Bank, 2022). Nevertheless, the increasing trend in urbanization represents a pressing sustainability concern, explicitly addressed by the Sustainable Development Goals. Cities have also been identified among the direct targets of the negative effects of climate change (UN-Habitat, 2011). Among others, the urban heat island effect (UHI) - which is identified where the temperature warming pattern is significantly higher than in the surrounding rural environment - has been largely recognized by the scientific community as a primary threat to human health and ecosystems (Heaviside et al., 2017). The UHI exposes citizens to continuous thermal stress while affecting local air circulation and rainfall patterns, thus contributing to air pollution (Xu et al., 2014) and risk of flooding (Hester and Bauman, 2013). In this context, measuring the effect of human activities on the UHI features a critical aspect to protect population and ecosystems' health through the implementation of adaptation and mitigation strategies.

In view of the above considerations, the employment of multiple geo-data sources is pivotal for a thorough understanding of the human footprint on local climate conditions. Several studies in the literature have addressed the analysis of this interaction by measuring the relationship between climate-related variables - namely air temperature and/or Land Surface Temperature (LST) - and land use/land cover (LULC) composition (Puche et al., 2023). While air temperature measurement is traditionally performed through ground sensor networks, LST can be monitored with remotely sensed thermal data. Ground sensors allow for high frequency measures while preventing a high spatial resolution which is demanded to investigate local-scale temperature patterns. Accordingly, most studies have focused on the analysis of LST rather than air temperature (Bokaie et al., 2016). This may appear as a limitation for UHI assessment purposes. However, some studies have revealed that LST can be used as a proxy of air temperature (Goldblatt et al., 2021), despite the relation between these variables depends on local weather conditions and surface characteristics while varying between day-time and night-time (Zhu et al., 2013).

Focusing on LST, literature findings show that this variable is directly influenced by a number of factors including vegetation, soil content, presence of pervious and impervious surfaces, and construction material used in roads and buildings (Weng and Lu, 2008). Specifically, while vegetation is the most accountable mitigating factor of LST in urban areas (Alavipanah et al., 2015), buildings and roads have been identified as the surface types experiencing the highest LST values, primarily due to the increased heat storage capability of their construction materials (Zhao et al., 2017). Despite this well-established framework, the LULC-LST relationship may significantly vary according to the background climate, with temperature differences generally decreasing with increasing background temperature (He et al., 2019).

With this in mind, this work provides insights into the effect of a motorway construction on the local LST patterns. The study is focused on the motorway A58 and connected roads and highways in the Metropolitan City of Milan (northern Italy). This experiment was designed with the goal of finding evidence of

* Corresponding author

the persistence of higher LST within the road and lower temperatures in the surrounding buffers characterized by a mixture of natural and artificial land cover composition. Observations from the Landsat 5 and Landsat 8 thermal cameras for the period 2006-2022 were exploited for measuring the LST space-time patterns. Statistics and graphs were computed to draw conclusions about the influence of the new motorway on the local temperature distribution. Results show a marked increase in LST along the road track and surrounding area which is more pronounced in summer than in winter.

The paper continues as follows. Section 2 describes the selected study area and time period for the analysis, as well as the data used to carry out the experiment. Section 3 illustrates data processing and results providing maps, graphs and statistics. Conclusions and future work are outlined in Section 4.

2. CASE STUDY DEFINITION

2.1 Study area and time period

The case study selected for this work is located in the Metropolitan City of Milan (northern Italy). This area is one of the most densely populated European regions, affected by poor wind circulation and dense urbanization favouring the persistence of a well-known urban heat island (Bacci and Maugeri, 1992). With the aim of assessing how urbanization can affect the local climate characteristics, a preliminary investigation of the changes over time in land consumption was carried out. This allowed us to define a suitable study area and time range for the analysis.

Data distributed by the Italian Institute for the Environmental Protection and Research (ISPRA, `https://www.isprambiente.gov.it/it/banche-dati`) was exploited for this purpose. Specifically, the dataset *Carta Nazionale Consumo di Suolo* (`https://groupware.sinanet.isprambiente.it/uso-copertura-e-consumo-di-suolo/library/consumo-di-suolo/`) depicts the spatial distribution of artificial surfaces (e.g., roads, railways, industries, and airports) at 10 m resolution. Data is available for the years 2006 and 2012 and with yearly frequency starting from 2015. By comparing the artificial surface coverage over the years, the detection of land consumption changes across the Metropolitan City of Milan was straightforward. The most appreciable change is represented by the construction of the motorway A58 *Tangenziale Est Esterna di Milano* (`https://www.tangenziale.esterna.it/`) in June 2012. Accordingly, the eastern part of the Metropolitan City of Milan was selected as a study area. Figure 1 depicts the extent of the area of interest and shows the path of the A58 and connected highways.

LST distribution was computed along the motorway track, in its neighbouring buffers (of 30 m and 120 m width) as well as in the whole area of interest. The time frame from 2006 to 2022 was split into two periods, namely 2006-2012 (before the motorway construction) and 2013-2022 (after the motorway construction). Data from the two time periods were compared to extract knowledge on the effect of the infrastructure on the LST space-time patterns, as explained in the following sections.

2.2 Landsat data

LST measurements were retrieved from the Landsat 5 and Landsat 8 missions to guarantee a number of satellite acquisitions over the whole study period. Landsat 5 was launched in March

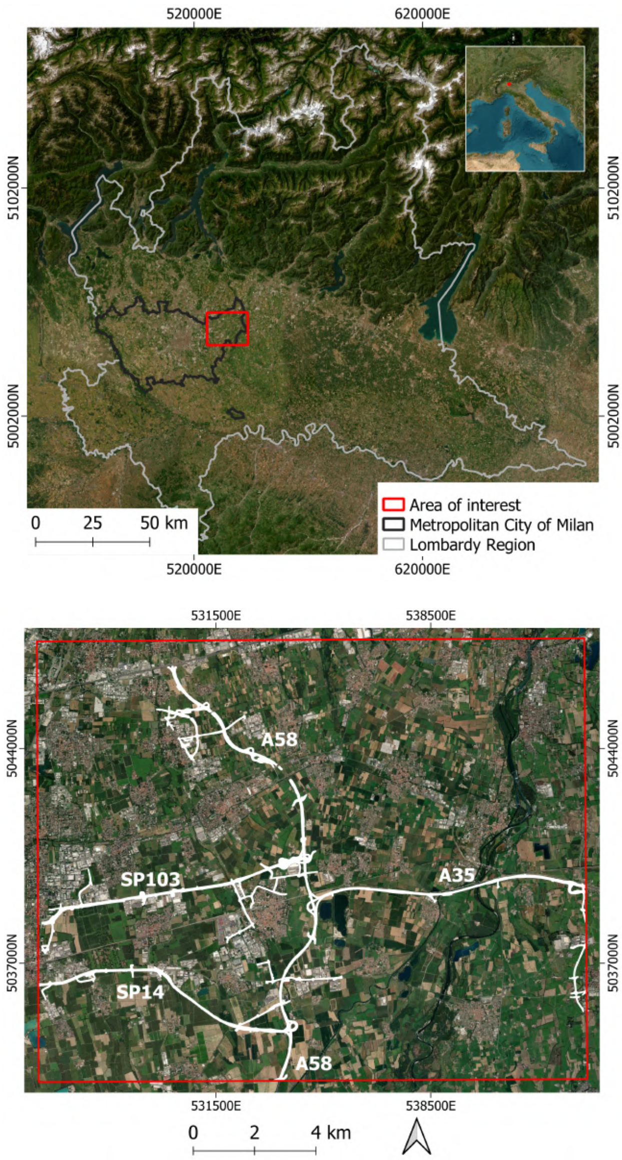

Figure 1. Location of the motorway A58 and connected highways within the study area. Coordinate reference system (CRS): WGS84/UTM zone 32N. Basemap data: © Esri Satellite.

1984 and was decommissioned after 29 years, in June 2013. Its Thematic Mapper (TM) acquired data in 7 spectral bands, including a thermal band (Band 6) at 120 m resolution. Data was distributed with global coverage and revisit time of 16 days (`https://www.usgs.gov/landsat-missions/landsat-5`). Landsat 8 was launched in February 2013 and is equipped with an Operational Land Imager (OLI) acquiring data in 9 optical bands as well as a Thermal Infrared Sensor (TIRS) which acquires data in 2 thermal bands (Band 10 and Band 11) with 100 m resolution. Landsat 8 collects images of the Earth every 16 days (`https://www.usgs.gov/landsat-missions/landsat-8`). For both satellites, data is provided in GeoTIFF format with an open-data license and is freely distributed by the United States Geological Survey (USGS) through its Earth Explorer (`https://earthexplorer.usgs.gov/`).

To compare the influence of the motorway on the LST distribution in the cold and warm seasons, one winter and one summer satellite acquisitions per year were downloaded, according to the satellite revisiting time and weather conditions. Due to the climate of the study area which is often characterized by foggy weather or low-clouds coverage during the cold season, the availability of winter acquisitions with adequate visibility was quite limited. The acquisition dates are reported in Table 1 and Table 2 for Landsat 5 and Landsat 8, respectively. For both sensors, the acquisition time is around 10:10 AM GMT+0 (GMT, Greenwhich Mean Time) according to the satellite sun-synchronous orbits.

Year	Summer	Winter
2006	13-07-2006	n.a.
2007	16-07-2007	n.a.
2008	n.a.	n.a.
2009	06-08-2009	n.a.
2010	09-08-2010	29-01-2010
2011	28-08-2011	31-12-2010
2012	n.a.	n.a.

Table 1. Acquisition date for Landsat 5 images (period before the motorway construction, i.e. from 2006 to 2012).

Year	Summer	Winter
2013	16-07-2013	07-12-2013
2014	19-07-2014	n.a.
2015	22-07-2015	n.a.
2016	25-08-2016	15-02-2016
2017	n.a.	16-01-2017
2018	30-07-2018	19-01-2018
2019	17-07-2019	06-01-2019
2020	19-07-2020	n.a.
2021	n.a.	11-01-2021
2022	09-07-2022	14-01-2022

Table 2. Acquisition date for Landsat 8 images (period after the motorway construction, i.e. from 2013 to 2022).

For the purposes of the present study, the thermal bands of the two satellites were leveraged. For Landsat 8, Band 10 was chosen due to the calibration errors of Band 11, as widely suggested in the literature (García, 2021). Data is down-scaled by the data provider and made available at 30 m resolution. The Collection 2 Level 2 (C2L2) product was exploited since it provides analysis-ready Bottom-of-Atmosphere (BOA) temperature values, thereby not requiring land surface emissivity data for deriving a LST estimation. Specifically, LST $[K]$ can be computed by simply rescaling the Digital Numbers (DN) according to the following equation:

$$LST = 0.00341802 * DN + 149, \quad (1)$$

as reported in the Landsat Product specifications. LST is then transformed into Celsius degrees [$°C$] by subtracting 273.15.

3. EFFECT OF THE MOTORWAY ON LAND SURFACE TEMPERATURE PATTERNS

3.1 Data processing

LST was computed for each acquisition date, resulting in 13 maps for summer (5 before and 8 after the road construction), and 9 maps for winter time (2 before and 7 after the road construction). Given the high number of Landsat images, data processing was carried out through a custom Python code taking advantage of popular libraries such as Pandas (`https://pandas.pydata.org`), Geopandas (`https://geopandas.org`), and Rasterio (`https://pypi.org/project/rasterio/`). Custom functions were developed for satellite imagery clipping, statistics computation, and results plotting.

As a first experiment, date-specific LST maps were averaged to derive the mean LST distribution per season (winter and summer) and time period (before and after road construction). Pixels falling within the road track and in the surrounding buffers of 30 m and 120 m width were then extracted to assess the effect of the highway on the LST distribution in the neighbouring areas. LST statistics including mean, median, standard deviation, and quartiles were computed for the motorway track and surrounding buffers as well as for the whole area of interest, distinguishing between the two seasons and time periods. Statistics were summarized and represented through boxplots.

As a second step, the difference in terms of LST between the period after and before the motorway construction was computed for both summer and winter. Similarly to the former experiment, statistics for the pixels over the road track, the buffers, and the whole area of interest were computed and displayed through boxplots. This test enabled the detection of the persistent change in LST distribution owing to the road construction regardless of the overall temperature difference between the two periods which may be due to different background climate conditions.

3.2 Results

The mean LST maps per period are reported in Figure 2 and Figure 3 for summer and winter, respectively. The evident overall increase in mean summer LST after the road construction may be attributed to a baseline temperature increase as well as the expansion of the urban centres towards the rural environment (see Figure 2). Also, the effect of the motorway construction can be detected as a visible increase of LST along the road paths. The same considerations cannot be outlined for the winter season (see Figure 3). In fact, the motorway track is not distinguishable from the surrounding, indicating a far lower influence of the road on LST distribution in the cold season. Furthermore, an overall significant increase in mean winter LST is exhibited in the period 2013-2022 due to different climatic conditions.

The above insights are confirmed by the boxplots reported in Figure 4 for summer and Figure 5 for winter. Few variations in the median LST are recorded before the road construction in the different zones. Median variations in LST are within 0.5°C and 0.1°C in summer and winter, respectively. After the motorway construction, a significant increase in median summer time LST is experienced along the road layout (+2.5°C with respect to the whole area of interest) as well as in the surrounding buffers, with decreasing temperature as the distance from the road increases (+2.1°C and +1.1°C within the 30 m and 120 m width buffers). Contrarily the increase in LST is negligible in the winter season. Boxplots also outline a lower dispersion of LST distribution along the road due to the homogeneous construction material compared to the heterogeneous land cover of the whole area of interest.

Furthering the data exploration, the difference of mean LST between the period after and before the road construction was computed. This experiment was intended to highlight the effect of the motorway construction independently of the different context climate conditions that may have been experienced in the two periods. The seasonal maps of LST differences are represented in Figure 6 which confirm the above considerations. Indeed, the road track is well-distinguishable in summer, indicating a significant increase in LST due to the motorway construction. Such influence is not visible for the winter map.

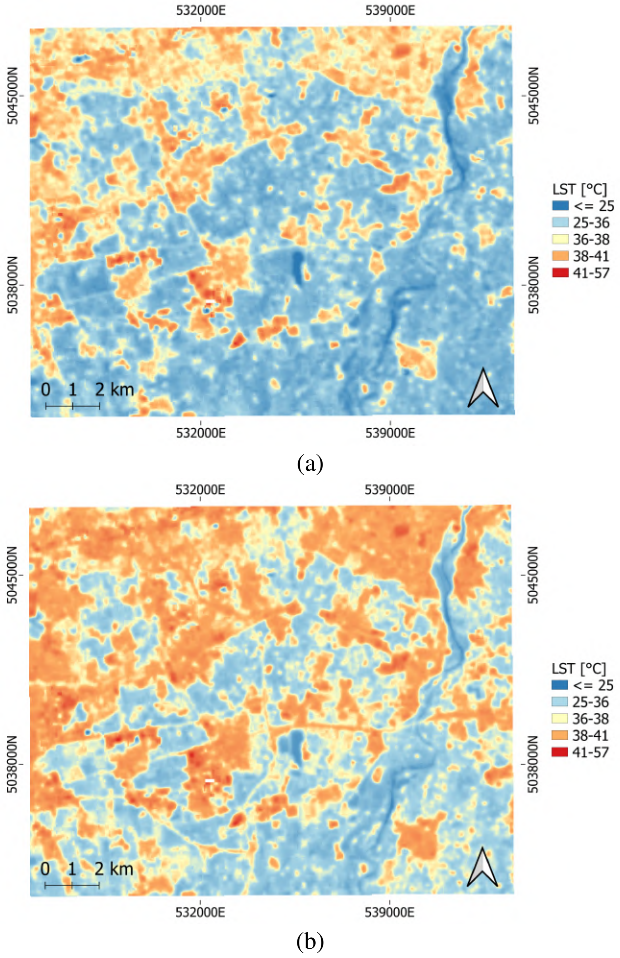

Figure 2. Mean summer LST distribution in the area of interest, (a) before and (b) after the motorway construction. CRS: WGS84/UTM zone 32N.

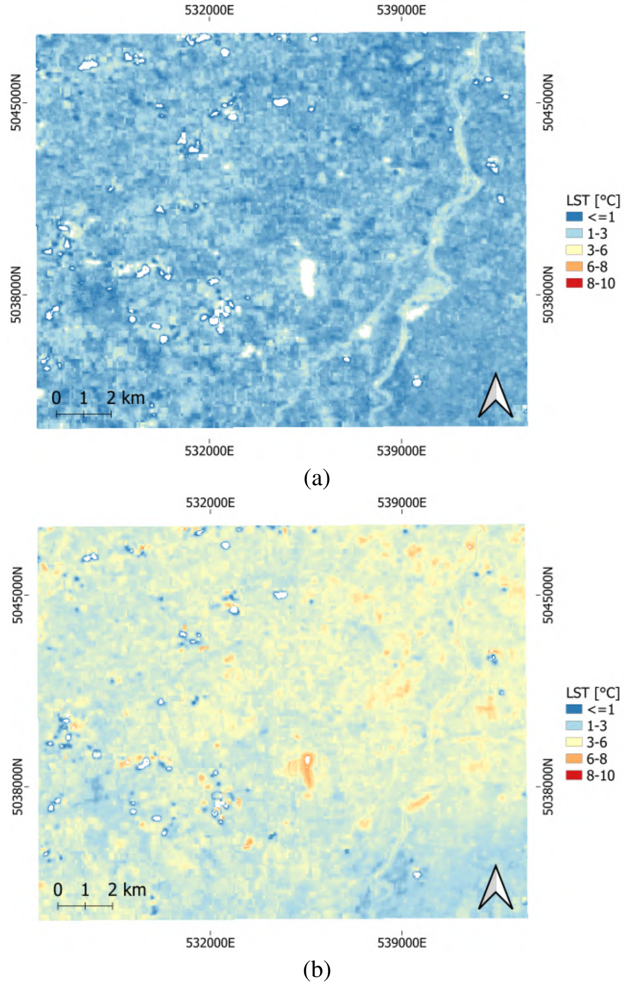

Figure 3. Mean winter LST distribution in the area of interest, (a) before and (b) after the motorway construction. CRS: WGS84/UTM zone 32N.

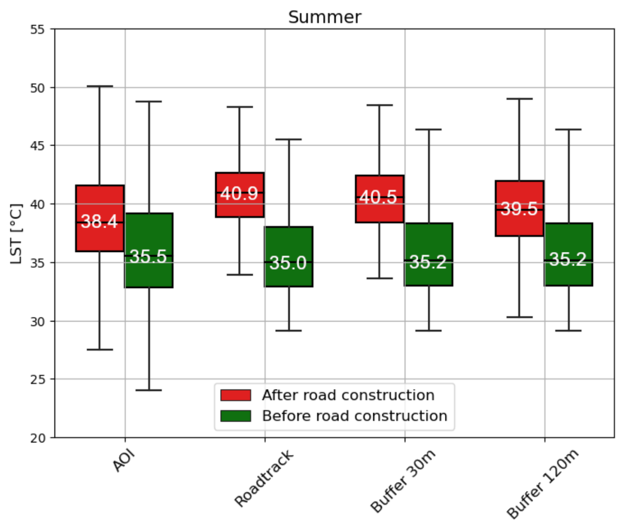

Figure 4. Boxplots of the mean summer time LST distributions for the whole area of interest (AOI), the road (roadtrack), and for the 30m (buffer 30m) and 120m (buffer 120m) width road buffers, before and after the motorway construction.

The seasonal distribution of mean LST difference is also displayed through boxplots in Figure 7. Beside a lower dispersion in winter, boxplots point out a major effect of the motorway along both its layout and buffer areas during summer. The median LST difference along the road is 5.1°C, i.e., 2.4°C higher than in the whole area of interest. A significant difference is also recorded along the 30 m and 120 m width buffers (+1.9°C and +0.7°C respectively compared to the whole area).

4. CONCLUSIONS

In the present study, the influence of a motorway construction on LST space-time patterns was measured using Landsat thermal data. The analysis focused on the motorway A58 and connected roads and highways which are located in the Eastern part of the Metropolitan City of Milan (northern Italy). The time frame considered for the investigation, ranging from 2006 to 2022, was split into two periods, namely before and after the motorway construction, to define a framework for assessing the motorway influence on LST.

Data acquired by the thermal cameras of Landsat 5 and Landsat 8 satellites were exploited to compute the LST in the area of interest. Several winter and summer cloud-free acquisitions of the two satellites were collected and averaged to obtain mean seasonal LST maps for the two time periods. LST distribution

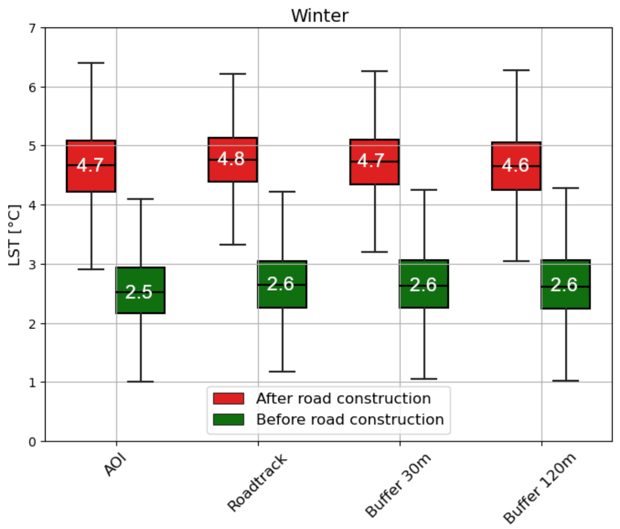

Figure 5. Boxplots of the mean winter time LST distributions for the whole area of interest (AOI), the road (roadtrack), and for the 30m (buffer 30m) and 120m (buffer 120m) width road buffers, before and after the motorway construction.

was explored and compared along the road track as well as in the neighbouring areas (buffers of 30 m and 120 m width) to provide insights into the influence of the infrastructure on the local surface temperature patterns.

Results show that the motorway experiences way higher LST values compared to the whole area of interest during summer. The surrounding buffers are partially affected by the motorway warming effect, with decreasing temperature values with increasing distance from the infrastructure. The winter LST distributions do not show the same pattern. On the contrary, the road effect on LST is quite dampened and the temperature excursion across the study area is more limited. This result may be attributed to the lower incident solar radiation which is among the primary responsible for high surface temperature values.

Disclosures provide pieces of evidence on the role played by artificial surfaces on the local climate while providing valuable insights for urban heat island mitigation strategies. Indeed, the metrics obtained in this study could be exploited by urban planners as a valuable tool for implementing policies connected, for example, to the use of vegetation alongside road paths for buffering temperature extremes in urban areas. Despite the assessment of heat islands should also consider air temperature - which is in fact an indicator of the local atmospheric conditions and thermal comfort - the combined analysis of LST and air temperature is not so trivial due to the poor availability and granularity of in-situ sensors. Future activities may be devoted to the installation of permanent air temperature sensors and/or to the collection of air temperature observations through in-situ surveys. This will allow understanding whether the infrastructure affects the air temperature patterns as well as measuring the magnitude of such effect.

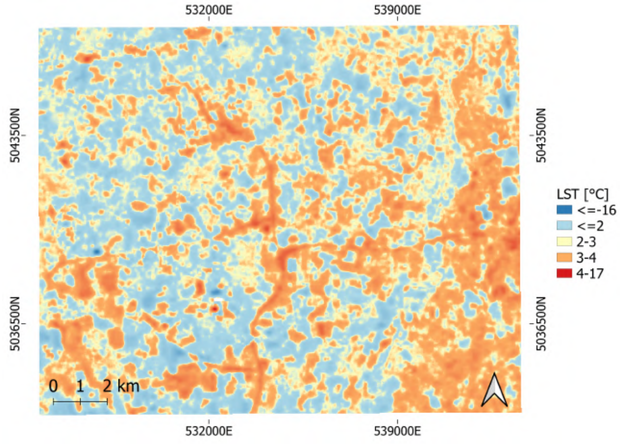

(a)

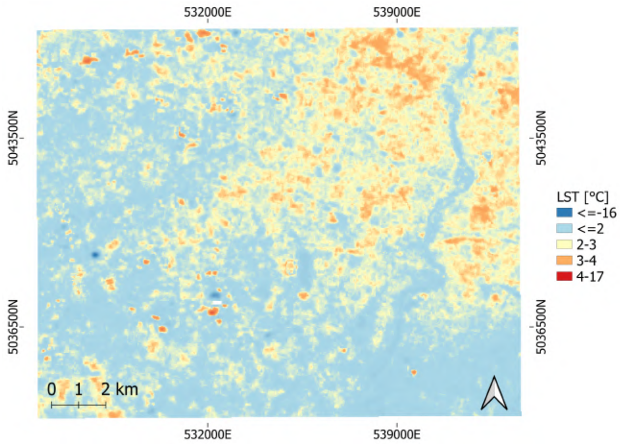

(b)

Figure 6. Mean LST difference between the period after and before the motorway construction relative to (a) summer and (b) winter. CRS: WGS84/UTM zone 32N.

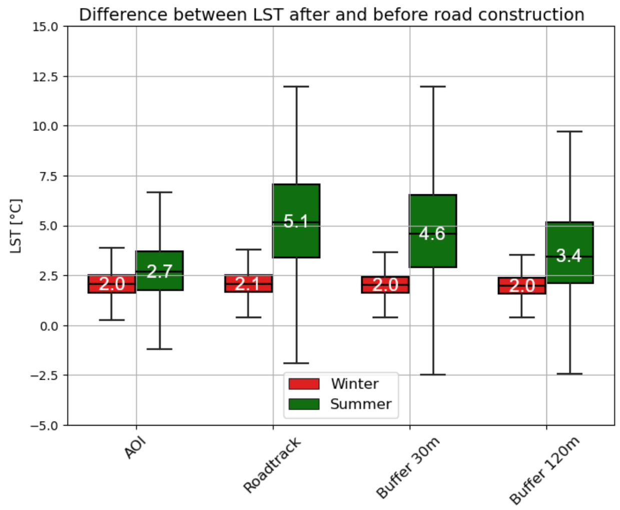

Figure 7. Boxplots of the mean LST difference between the period after and before the motorway construction for the whole area of interest (AOI), the road (roadtrack), and for the 30m (buffer 30m) and 120m (buffer 120m) width road buffers.

REFERENCES

Alavipanah, S., Wegmann, M., Qureshi, S., Weng, Q., Koellner, T., 2015. The Role of Vegetation in Mitigating Urban Land Surface Temperatures: A Case Study of Munich, Germany during the Warm Season. *Sustainability*, 7(4), 4689–4706.

Bacci, P., Maugeri, M., 1992. The urban heat island of Milan. *Il Nuovo Cimento C*, 15, 417–424.

Bokaie, M., Zarkesh, M. K., Arasteh, P. D., Hosseini, A., 2016. Assessment of Urban Heat Island based on the relationship between land surface temperature and Land Use/ Land Cover in Tehran. *Sustainable Cities and Society*, 23, 94–104.

García, D. H., 2021. Analysis and precision of the Terrestrial Surface Temperature using Landsat 8 and Sentinel 3 images: Study applied to the city of Granada (Spain). *Sustainable Cities and Society*, 71, 102980.

Goldblatt, R., Addas, A., Crull, D., Maghrabi, A., Levin, G. G., Rubinyi, S., 2021. Remotely Sensed Derived Land Surface Temperature (LST) as a Proxy for Air Temperature and Thermal Comfort at a Small Geographical Scale. *Land*, 10(4), 410.

He, B.-J., Zhao, Z.-Q., Shen, L.-D., Wang, H.-B., Li, L.-G., 2019. An approach to examining performances of cool/hot sources in mitigating/enhancing land surface temperature under different temperature backgrounds based on landsat 8 image. *Sustainable Cities and Society*, 44, 416–427.

Heaviside, C., Macintyre, H., Vardoulakis, S., 2017. The Urban Heat Island: Implications for Health in a Changing Environment. *Current Environmental Health Reports*, 4(3), 296–305.

Hester, E. T., Bauman, K. S., 2013. Stream and Retention Pond Thermal Response to Heated Summer Runoff From Urban Impervious Surfaces. *Journal of the American Water Resources Association*, 49(2), 328–342.

Puche, M., Vavassori, A., Brovelli, M. A., 2023. Insights into the Effect of Urban Morphology and Land Cover on Land Surface and Air Temperatures in the Metropolitan City of Milan (Italy) Using Satellite Imagery and In Situ Measurements. *Remote Sensing*, 15(3), 733.

UN-Habitat, 2011. Cities and Climate Change: Global Report on Human Settlements 2011. UN-Habitat, United Nations Human Settlements Programme, Nairobi, Kenya.

United Nations, 2018. World urbanization prospects: The 2018 revision. Available online: `https://population.un.org/wup/` (accessed on 17th February 2023).

Weng, Q., Lu, D., 2008. A sub-pixel analysis of urbanization effect on land surface temperature and its interplay with impervious surface and vegetation coverage in Indianapolis, United States. *International Journal of Applied Earth Observation and Geoinformation*, 10(1), 68–83.

World Bank, 2022. Urban development. Available online: `https://www.worldbank.org/en/topic/urbandevelopment/overview` (accessed on 17th February 2023).

Xu, L.-Y., Yin, H., Xie, X.-D., 2014. Health Risk Assessment of Inhalable Particulate Matter in Beijing Based on the Thermal Environment. *International Journal of Environmental Research and Public Health*, 11(12), 12368–12388.

Zhao, Z.-Q., He, B.-J., Li, L.-G., Wang, H.-B., Darko, A., 2017. Profile and concentric zonal analysis of relationships between land use/land cover and land surface temperature: Case study of Shenyang, China. *Energy and Buildings*, 155, 282–295.

Zhu, W., Lű, A., Jia, S., 2013. Estimation of daily maximum and minimum air temperature using MODIS land surface temperature products. *Remote Sensing of Environment*, 130, 62–73.